Canadian Mineralogist
Vol. 31, pp. 185-202 (1993)

THE FELDSPARS OF THE SIERRA ALBARRANA GRANITIC PEGMATITES, CORDOBA, SPAIN

MARIA DEL MAR ABAD-ORTEGA, PURIFICACION FENOLL HACH-ALI, JOSE DANIEL MARTIN-RAMOS AND MIGUEL ORTEGA-HUERTAS

Departamento de Mineralogía y Petrología, Universidad de Granada, Instituto Andaluz de Geología Mediterránea, C.S.I. 18002 Granada, Spain

ABSTRACT

The feldspars from granitic pegmatites of the Sierra Albarrana Lower Paleozoic complex (Córdoba, Spain) are present i following structural states: orthoclase, low and intermediate microcline, the latter being the most abundant of the three, as rev by an X-ray-diffraction study (powder method). The Al–Si distribution is quite ordered, with triclinic phases of interme triclinicity, and moderate degree of order, together with highly ordered phases, whereas only two samples are more disor and have monoclinic symmetry. The Al–Si distribution seems to follow an intermediate trend between a one-step and a two path of ordering. The geochemical data show that in the successive generations of feldspars, the Or and An contents decr whereas the Ab content increases. In the same way, the P, Rb and Cs contents increase, whereas the Sr and Ba contents decr Pb presents an erratic behavior. Toward the center of the pegmatite, t_1o value increases, and t_1m and $2t_2$ decrease. The feld reveal the development of the magmatic, subsolidus and hydrothermal stages of crystallization of Parsons & Brown (1984) first stage is demonstrated by the metastable persistence of disordered monoclinic feldspar (orthoclase). During the subso stage, triclinic feldspar appears with an intermediate degree of order and the development of vein-textured and braided pe and albite–pericline twinning. K-feldspar with a high degree of order (close to the low microcline end-member) an development of patch perthite are indicative of the hydrothermal stage.

Keywords: feldspars, granitic pegmatites, X-ray diffraction, powder method, Al–Si order, orthoclase, microcline, Sierra Alba Spain.

SOMMAIRE

Une étude par diffraction X sur poudres de feldspath perthitique provenant de pegmatites granitiques du complexe paléoz de Sierra Albarrana, à Córdoba, en Espagne, démontre la présence de l'orthose, du microcline ordonné et du micro intermédiaire, le plus abondant. La distribution Al–Si est relativement bien ordonnée; la plupart des échantillons contienne feldspath triclinique à "triclinicité" intermédiaire, et montrent une association de celui-ci avec un microcline très bien ord tandis que seulement deux échantillons contiennent un feldspath monoclinique, et donc plus désordonné. La distribution de Si semble poursuivre une évolution intermédiaire entre une transition à une étape et à deux étapes. Les données géochim montrent que dans les générations successives de feldspaths, la teneur en Or et en An diminue, tandis que la teneur en Ab augm De la même façon, la teneur en P, Rb et Cs augmente, tandis que celle en Sr et Ba diminue. Le Pb a un comportement erra La valeur de t_1O augmente vers le coeur de la pegmatite, et t_1m et $2t_2$ diminuent. Les grains de feldspath montrent un développe magmatique et des modifications subsolidus et hydrothermales (Parsons & Brown 1984). Le premier stade de cristallisati partiellement préservé dans l'orthose. Au cours du stade subsolidus, le feldspath triclinique à degré d'ordre intermédiaire son apparition, de même qu'une texture perthitique en veines et en tresses et les macles albite–péricline. Le feldspath potas à degré d'ordre élevé, près du pôle microcline ordonné, et le développement de perthite en taches sont les manifestations du hydrothermal.

(Traduit par la Réda

Mots-clés: feldspaths pegmatites granitiques, diffraction X, méthode des poudres, degré d'ordre Al–Si, orthose, microcline, Albarrana, Espagne.

INTRODUCTION AND GEOLOGICAL CONTEXT

The pegmatite deposits of Sierra Albarrana, of Hercynian age according to Azor *et al.* (1991), are located in the northern part of the province of Córdoba, near the town of Fuenteobejuna, in the southwestern part o Iberian Massif, in the Ossa Morena zone (Chacón 1974, Garrote 1976, Eguiluz 1987, Azor *et al.* (Fig. 1A). The host rocks (Fig. 1B) are Lower Palec rocks belonging to three distinct complexes (Garr

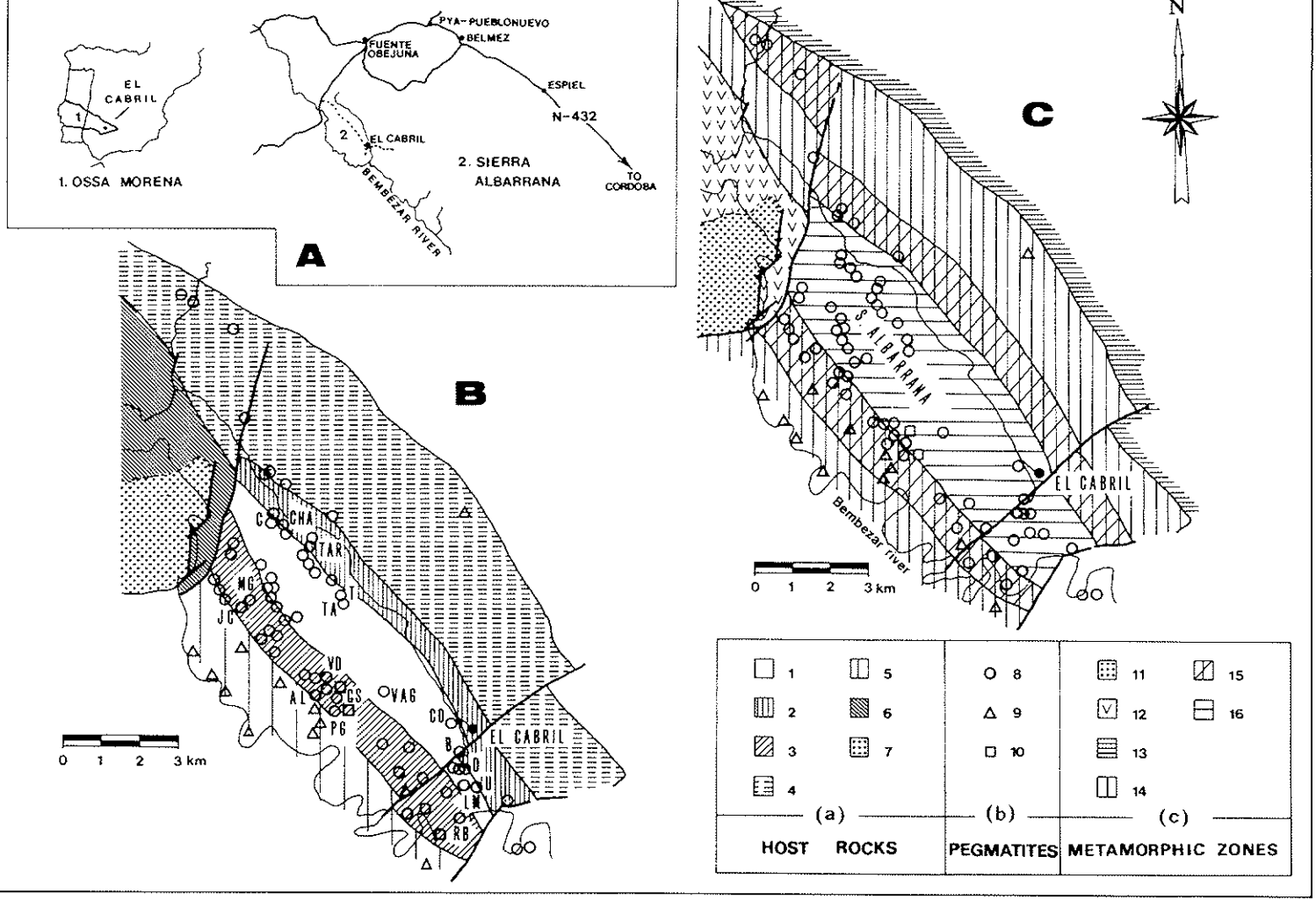
PYA-PUEBLONUEVO
BELMEZ
FUENTE OBEJUNA
ESPIEL
N-432
TO CORDOBA
EL CABRIL
1
2
1. OSSA MORENA
2. SIERRA ALBARRANA
BEMBEZAR RIVER
A
B
C
N
S. ALBARRANA
EL CABRIL
Bembezar river
0 1 2 3 km
CHA
TAR
MG
JC
TA
VD
AL
GS
PG
VAG
CD
B
LN
RB
1
2
3
4
5
6
7
8
9
10
11
12
13
14
15
16
(a)
HOST ROCKS
(b)
PEGMATITES
(c)
METAMORPHIC ZONES

TABLE 1. CHARACTERISTIC OF PEGMATITES AND HOST ROCKS

	PEGMATITES				HOST - ROCKS	
	TYPE	SHAPE & DIMENSIONS	NUMBER OF BODIES	MINERALOGY	METAMORPHISM	LITHOLOGY
I.	AMPHIBOLE-EPIDOTE PEGMATITES	Irregular bodies (1 - 100 cm)	2	Amph, Ep, Ab, Tur	Sil - K-Fd	Amphibolites and amphobolitic gneisses
II.	Al-SILICATE PEGMATITES	Irregular bodies (1 - 100 cm) or tabular masses (max. length = 1 m; max. width = 20 cm)	10	Q, And, Sil, Ms, Bt, Chl	Sil - K-Fd Sil - Ms St - And	Muscovite schists
III.	QUARTZ-FELDSPAR PEGMATITES	Irregular and tabular masses (max. length = 550 m; max. width = 100 m)	60	Q, K-Fd, Ab, Ms, Tur, Grt, Bt, Brl, Cbrl, Chl, Rt, Ap, Zrn, Py, Mag, Ilm, U minerals	Sil - K-Fd Sil - Ms	Feldespar quartzites and gneisses

Amph= amphibol, Ep = epidote, Ab = albite, Tur = tourmaline, Q = quartz, And = andalucite, Sil = sillimanite, Ms = muscovite, Bt = biotite, Chl = chlorite, K-Fd = K-feldspar, Grt = garnet, Brl = beryl, Cbrl = chrysoberyl, Rt = rutile, Ap = apatite, Zrn = zircon, Py = pyrite, Mag = magnotite, Ilm = ilmenite, St = staurolite.

al. 1980, Ortega-Huertas *et al.* 1982, Azor *et al.* 1991): 1) a succession of metamorphic rocks: quartzites, gneisses, schists, amphibolites and metabasites (Chacón *et al.* 1974, Garrote 1976, Delgado-Quesada *et al.* 1977, Quesada *et al.* 1990) (Fig. 1B, 1 to 6), 2) continental-type conglomeratic sediments, with abundant clasts of metamorphic rocks, lava flows and pyroclastic materials, which unconformably overlie the metamorphic rocks (Garrote & Sánchez-Carretero 1983, Gabaldón *et al.* 1983) (Fig. 1B, 7), and 3) postmetamorphic igneous rocks including the Alcornocal volcanic complex and the granitic stock of La Cardenchosa (Delgado-Quesada 1971).

A metamorphic zonation has been recognized in the Sierra Albarrana area (Garrote 1976): from high to low grade, sillimanite – K-feldspar, sillimanite–muscovite, staurolite–andalusite, garnet, biotite and chlorite (Fig. 1C). The distribution of pegmatites (Figs. 1B, C) is controlled by this metamorphic zonation. The pegmatites appear only in the three higher-grade zones.

The morphology and types of pegmatites are summarized in Table 1 according to their mineralogical composition and the characteristics of the host rocks. The feldspars described here are from type-III granitic pegmatites (Table 1). As these pegmatites do not contain a typical quartz core, we have only been able to establish the following zonation from border to center and from top to bottom of the pegmatite bodies in some outcrops (Cerro de la Sal, Peña Grajera, Juan Calvillo: Figs and 4).

1) Border zone (zone 2, Figs. 2–4): medium-gr pegmatites of granitic texture, whose size incr gradually inward. This zone contains quartz and per feldspar and is rich in tourmaline, garnet, chl muscovite and arborescent biotite.

2) Wall zone (zone 3, Figs. 2–4): coarse-grained, a graphic texture, containing quartz, K-feldspar, and minor muscovite.

3) Intermediate zone or Central zone (zone 4, Fi 4; zone 3, Fig. 3): very coarse-grained (crystals o to two meters) and giant pegmatitic texture, mainly up of quartz and K-feldspar.

METHODOLOGY

Feldspar samples were collected from the prin type-III pegmatites in the following outcrops: Cer la Sal, Peña Grajera, Diéresis, Los Morales, Un Colmenar, Beta, Coma, Cruz de Chaparral, Trav Taravilla, Valverda, Alameda, Valdenoque, Calvillo, Pozos de Juan Calvillo, Río Bembezar Fuenteobejuna (Figs. 1B, 2, 3 and 4). All outcrop irregular, tabular masses (Table 1).

The optical and textural characterization of the p sic feldspar and plagioclase was carried out by stu

FIG. 1. (A) Geographic location of Sierra Albarrana. (B) Geology of Sierra Albarrana and location of the main pegm (modification of the map of Contreras *et al.* 1983). (C) Metamorphic zonation (modification of the results of Contreras 1983). (a) Host rocks: 1. Albarrana Formation: feldspathic quartzites with metapelitic layers, 2. Cabril Formation: gneisses, 3. Peña Grajera Formation: migmatitic gneisses, amphibolitic gneisses, amphibolites, 4. Montesina Form schists, 5. Bembezar Formation: schists, quartzites and metabasites, 6. Azuaga Formation: phyllites and metagreywack Valdinfierno Basin (Lower Carboniferous). (b) Pegmatites: 8. quartzofeldspathic pegmatites, 9. pegmatites with alum silicates, 10. pegmatites with amphibole or epidote (or both). Principal pegmatite quarries: Cerro de la Sal: CS, Peña Gr PG, Diéresis: D, Los Morales: LM, Umbría: U, Colmenar: CO, Beta: B, Coma: C, Cruz de Chaparral: CHA, Traviesas: TA, Taravilla: TAR, Valverda: VAG, Alameda: AL, Valdenoque: VD, Juan Calvillo: JC, Pozos de Juan Calvillo: MC Río Bembezar: RB. (c) Metamorphic zones: 11. Lower Carboniferous (postmetamorphic), 12. biotite and chlorite zon garnet zone, 14. staurolite–andalusite zone, 15. sillimanite–muscovite zone, 16. sillimanite – K-feldspar zone.

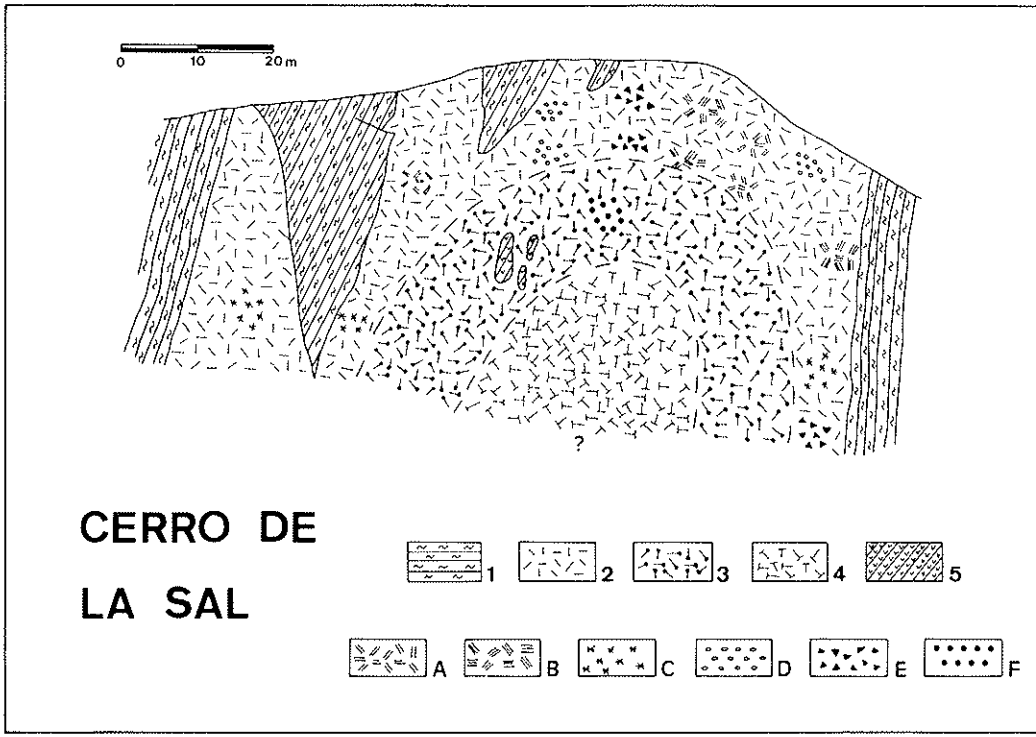

FIG. 2. Schematic cross-section of the Cerro de la Sal quarry showing internal zonation and location of samples: 1. Host r quartzitic gneisses, 2. Border zone: quartz–perthite pegmatite (granitic texture), 3. Wall zone: quartz–perthite pegr (graphic texture), 4. Intermediate zone: quartz – microcline – albite pegmatite (giant pegmatite structure), 5. chlo muscovite – garnet nodules. A. Muscovite, B. Biotite, C. Chlorite, D. Garnet, E. Tourmaline, F. Beryl.

thin sections, some of which were stained with sodium cobaltinitrite (after one minute etching with HF fumes).

Feldspar grains were separated manually (under the binocular microscope) and then ground in an agate mortar for an investigation of structural and compositional properties by X-ray diffraction (powder method). A Philips PW1710 diffractometer was used with Cu$K\alpha$ radiation, graphite monochromator and automatic slit. External standards of Si, CaF_2 and $KBrO_3$ were used in the calibration of the equipment. $KBrO_3$ also was used as an internal standard (in a 1:1 proportion with the feldspar).

Two diffractograms were made of each sample using the "POLVO" program of Martín-Ramos (1990) under the following experimental conditions: 40 kV, 40 mA, Recorder Full Scale = 1×10^3 counts per second, integration time = 0.6 s, and static record in order to avoid peak displacement. The first diffractogram was made between 27° and 32° 2θ, with a scanning speed of 1° 2θ/min and counts recorded every 0.012° 2θ in order to differentiate between monoclinic and triclinic K-feldspar by the profile of the 131 and $1\bar{3}1$ reflections; second (full) diffractogram was made between 3 80° 2θ, and counts recorded every 0.060° 2θ.

The results were interpreted using the "LECI routine ("POLVO" program, Martín-Ramos 1990) lowing the recommendations of Bish & Post (1989) resulting reflections were indexed according to the of Wright & Stewart (1968), Borg & Smith (1969 Ribbe (1983a). The crystallographic parameters refined by least squares using the program of Appl & Evans (1973) ("LSUCRE").

The triclinicity index was calculated followin formula of Goldsmith & Laves (1954). The degr Al–Si order was determined using: a) the meth Kroll & Ribbe (1987) derived from the $b - c^*$ and γ^* diagrams, b) on the basis of the translation dist in the [110] and [$1\bar{1}0$] directions following Kroll (1973, 1980) and Kroll & Ribbe (1987), c) on the of the "corrected" translations in the [110] and directions following Kroll & Ribbe (1987). The d of internal strain was determined following Stew

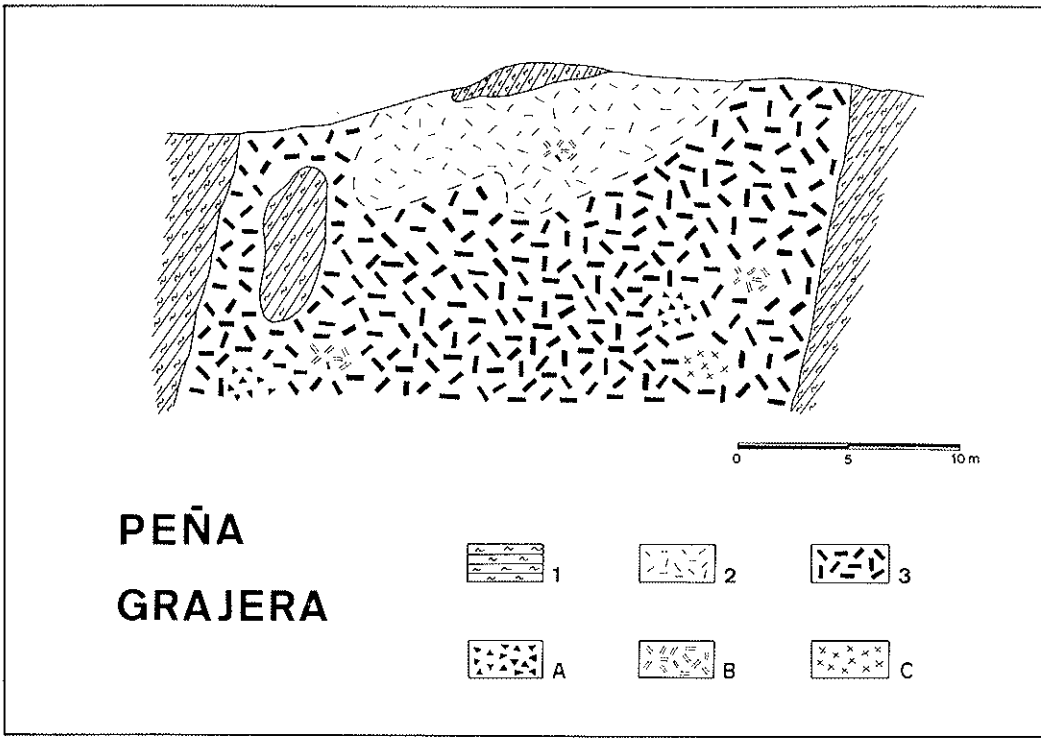

FIG. 3. Schematic cross-section of the Peña Grajera quarry showing internal zonation and location of samples: 1. Host r tourmalinized feldspathic schists and quartzitic gneisses, 2. Border zone: quartz–perthite pegmatite (granitic texture), 3. Ce zone: quartz – perthite – beryl pegmatite (giant pegmatite structure). A. Tourmaline, B. Muscovite, C. Quartz.

Wright (1974) (Δa parameter) and Kroll & Ribbe (1987) (*S.I.* parameter).

The degree of solid solution of each feldspar was estimated from refined unit-cell parameters, on the basis that strong modifications in *a* axis dimension and cell volume are related to slight changes in composition, according to Waldbaum & Thompson (1968), Kroll & Ribbe (1983), Kroll *et al.* (1986) (compositions estimated from cell volume) and Hovis (1986) (compositions estimated from cell volume and *a* dimension).

The chemical analyses were carried out at the X-Ray Assay Laboratories in Toronto, Ontario using X-ray fluorescence (Si, Al, Fe, Mg, Na, K, Ca, Ti, P, Ba, Rb), neutron activation (Cs, Au, U), Inductively Coupled Plasma (Mn, B, Be, Pb, Sr, Y) and wet chemistry. The analytical determinations using the electron-probe microanalyzer were carried out at the Université Paul Sabatier in Toulouse. On the basis of these data, possible temperatures of equilibration were obtained with model of Fuhrman & Lindsley (1988).

TEXTURAL, STRUCTURAL AND COMPOSITIONAL CHARACTERISTICS OF THE FELDSPARS

The K-feldspar in the type-III pegmatites has w pink or dark (blue or grey) coloring and a ma perthitic character. Following the nomenclatur Smith (1974), we found the perthite (Fig. 5) to ha vein texture (regular and irregular), which may grad change to either patch or braid perthite, and interloc perthite. Antiperthite is rare; the width of the albite l varies from 0.1 to 1.5 mm. The K-feldspar comm contains albite–pericline twinning, with twinned a coexisting in the same crystal with other appare untwinned areas. Plagioclase crystals are less abun

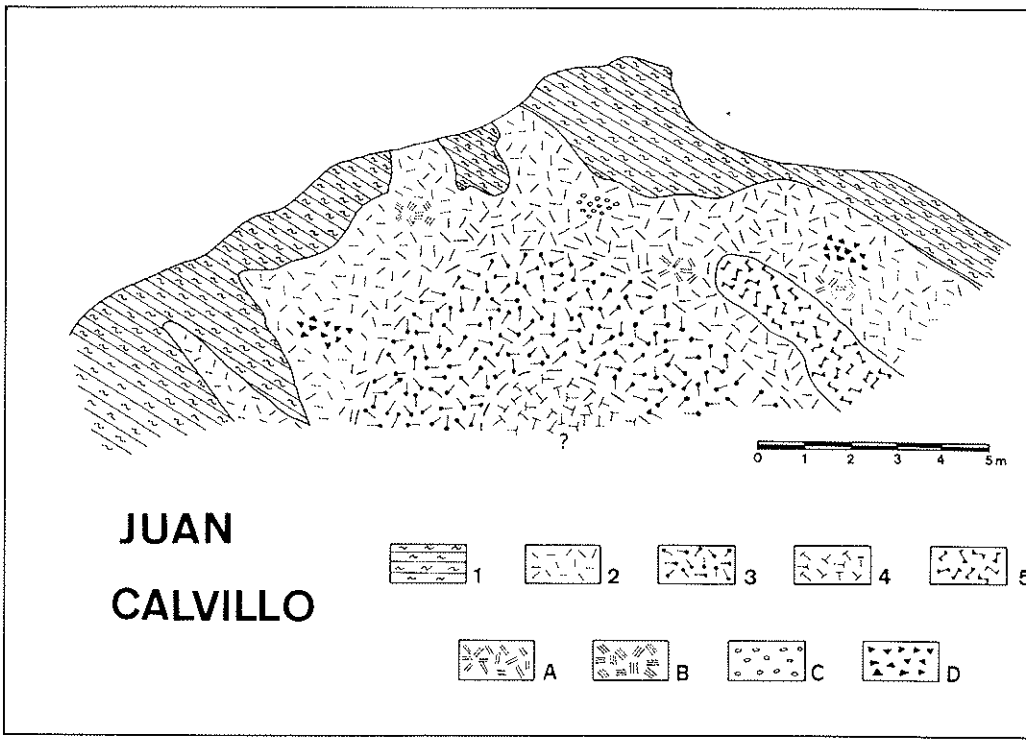

FIG. 4. Schematic cross-section of the Juan Calvillo quarry showing internal zonation and location of samples: 1. Host quartzitic gneisses and feldspathic schists, 2. Border zone: quartz–perthite pegmatite (granitic texture), 3. Wall quartz–perthite pegmatite (graphic texture), 4. Intermediate zone: quartz – microcline – albite pegmatite (giant peg structure), 5. Replacement body with biotite. A. Muscovite, B. Biotite, C. Garnet, D. Tourmaline.

than potassic feldspar, but invariably display polysynthetic twinning (Fig. 5e). Where they are juxtaposed, the K-feldspar seems to have replaced the plagioclase. Graphic K-feldspar – quartz intergrowths also are present.

The phases of K-feldspar detected by X-ray diffraction, following Ribbe (1983b) and McGregor & Ferguson (1989), indicate a wide variation in the structural state: orthoclase, intermediate microcline (much more abundant than the former), low microcline and low albite. Table 2 shows the refined crystallographic parameters of the different K-feldspar samples studied. Note the presence of the four structural states mentioned above.

Triclinicity ("obliquity") derived from the 131 and $1\bar{3}1$ reflections [$\Delta = 12.5(d_{131} - d_{1\bar{3}1})$: Goldsmith & Laves 1954)] ranges between 0.25 and 0.94 (Table 3), with a small additional monoclinic peak between reflections 131 and $1\bar{3}1$ in the samples with low triclinicity, due to the coexistence of both structural states (monoclinic and intermediate triclinicity). Values of triclinicity based from refined unit-cell parameters (Δ = measured $\gamma^* - 90°/2.29°$: McGregor & Ferguson 1989) are more reliable because of the large amount of low certainly present with the K-feldspar in the po samples analyzed by X-ray diffraction. No signi variations were found in the values of the degr Al–Si order obtained by the two different me (Tables 3, 4).

The $b - c^*$ diagram (Fig. 6) shows that the K-fel presents a moderately ordered Al–Si distribution two samples having monoclinic symmetry (PG–2c JC–1iz: Table 3), whereas the $\alpha^* - \gamma^*$ diagram (F shows the presence of the structural states ment above (orthoclase, intermediate microcline, low m cline). Similar conclusions can be deduced fro study of Figure 8 (Table 4), in which the coexister moderately ordered triclinic phases with interme triclinicity can clearly be seen, together with sa with a high degree of Al–Si order (close to that low microcline end-member).

The Al–Si distribution observed in most o samples seems to follow an intermediate tend between a one-step and a two-step distribution (Figs. 9, 10). However, two of the samples (PG–3c

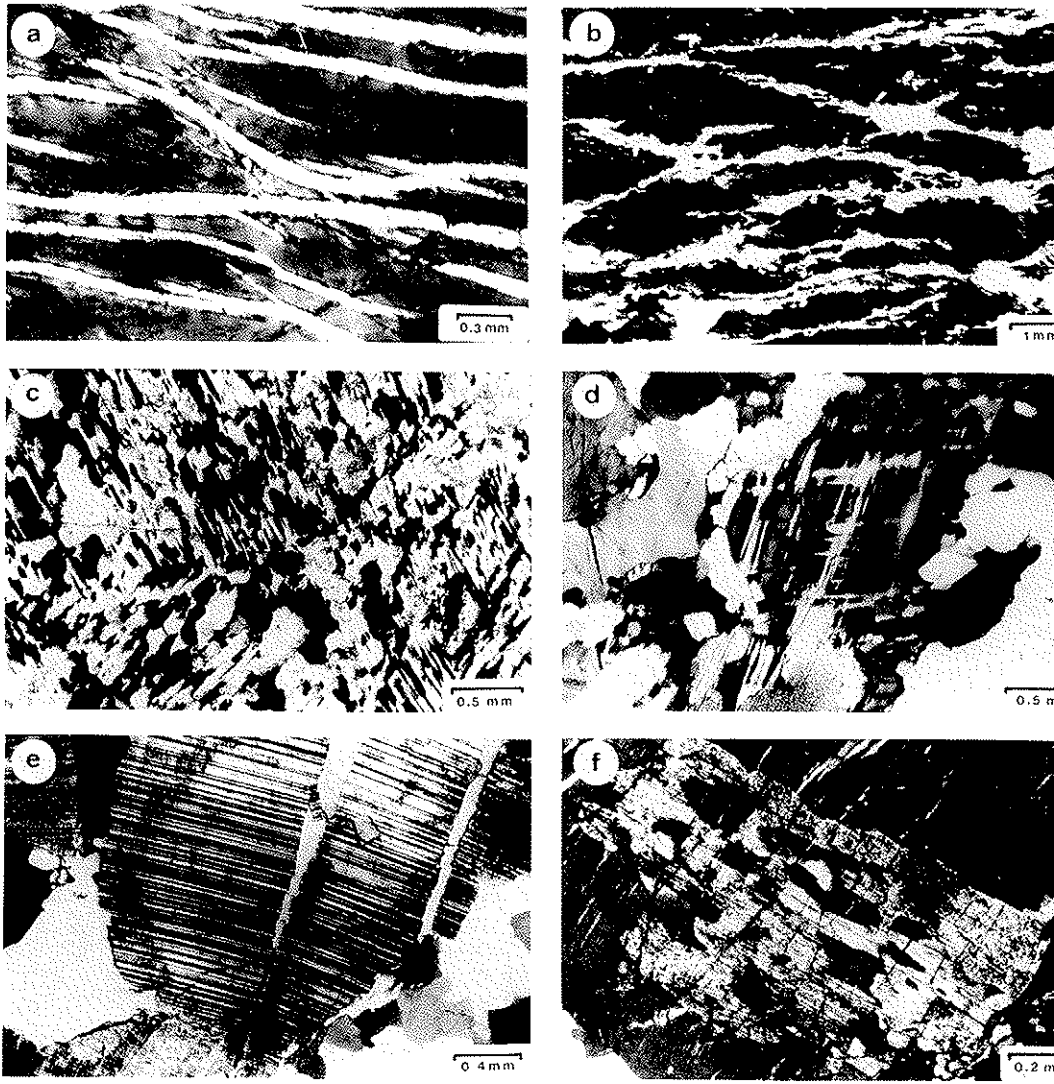

FIG. 5. Photomicrographs illustrating feldspar textures: (a) vein perthite, (b) patch perthite, (c) antiperthite (in a, b and c K-feldspar is dark, and plagioclase, light), (d) microcline: albite–pericline twinning, (e) albite: polysynthetic twinning (a law), and (f) coexisting K-feldspar (dark) and plagioclase (light); the K-feldspar seems to replace the plagioclase. All pl in cross-polarized light.

JC–1bz) show a highly ordered Al–Si distribution, close to the low microcline end-member.

Despite the limitations of the powder-diffraction method, we have attempted to determine the degree of strain in the cell. Some strain can be detected in the structure of most of the K-feldspar examined (Table 5): Δa varies from –0.108 to +0.154 (Table 5), *S.I.* from –20.03 to +11.50 (Table 5, Fig. 11). Such strain may be due to high Na contents in the bulk feldspars. It would also explain why many of the feldspar samples have anomalous parameters, since "strain" in the structure is associated with the exsolution of the Na-phase and inversion of symmetry, and is independent of the A distribution in each phase (Stewart & Wright 1 Eggleton & Buseck 1980). Therefore, since the feld studied here is markedly perthitic, the strain index r be rather high. According to Stewart & Wright (19 the higher degrees of internal strain could correspon feldspar with more sodium-rich overall compositi However, this hypothesis must be confirmed by tr mission electron microscopy.

The composition of the K-feldspar phase of

TABLE 2. REFINED CRYSTALLOGRAPHIC PARAMETERS OF POTASSIC FELDSPAR

SAMPLE	a(Å)	b(Å)	c(Å)	α(°)	β(°)	γ(°)	a*(Å)	b*(Å)	c*(Å)	α*(°)	β*(°)	γ*(°)	VOL(Å
CS-1bz	8.576(7)	12.981(7)	7.207(5)	90.36(6)	115.94(5)	89.10(5)	0.1297(1)	0.0770(1)	0.1543(1)	90.04(6)	64.06(5)	90.83(5)	721.4
CS-1wz	8.576(8)	12.990(9)	7.193(7)	90.03(9)	115.79(7)	89.36(9)	0.1295(1)	0.0770(1)	0.1544(1)	90.27(8)	64.21(7)	90.69(9)	721.5
CS-1iz	8.573(2)	12.982(2)	7.197(2)	89.81(5)	115.84(9)	89.52(9)	0.1296(3)	0.0770(1)	0.1544(2)	90.44(9)	64.16(9)	90.62(9)	720.9
CS-2iz	8.578(4)	12.970(3)	7.198(3)	90.06(9)	115.84(9)	88.88(9)	0.1296(6)	0.0771(2)	0.1544(3)	90.48(9)	64.16(9)	91.22(9)	720.6
PG-1bz	8.587(4)	12.936(3)	7.222(2)	90.06(9)	116.19(8)	88.76(9)	0.1298(6)	0.0773(2)	0.1543(2)	90.54(9)	63.81(9)	91.35(9)	719.7
PG-2bz	8.571(9)	12.965(9)	7.220(7)	90.28(6)	116.08(6)	88.94(9)	0.1299(1)	0.0771(1)	0.1542(1)	90.20(7)	63.92(6)	91.04(9)	720.5
PG-1cz	8.564(9)	13.010(9)	7.202(9)	90.23(9)	115.98(9)	89.43(9)	0.1299(2)	0.0769(1)	0.1545(2)	90.02(9)	64.02(9)	90.52(9)	721.2
PG-2cz	8.571(9)	13.015(9)	7.198(9)	90	116.14(7)	90	0.1300(1)	0.0768(1)	0.1547(1)	90	63.86(7)	90	720.9
PG-3cz	8.564(9)	12.950(9)	7.224(9)	90.42(9)	115.83(9)	87.90(9)	0.1298(1)	0.0773(1)	0.1538(2)	90.55(9)	64.17(9)	92.13(9)	720.6
JC-1bz	8.560(9)	12.964(9)	7.229(8)	90.62(8)	115.91(7)	87.86(9)	0.1300(2)	0.0772(1)	0.1538(1)	90.35(9)	64.10(7)	92.07(9)	721.1
JC-2bz	8.586(5)	12.983(8)	7.220(4)	90.17(5)	115.98(4)	89.22(6)	0.1296(1)	0.0770(1)	0.1541(1)	90.19(5)	64.02(4)	90.78(5)	723.4
JC-1wz	8.597(9)	12.948(9)	7.202(9)	90.30(9)	116.00(9)	89.24(9)	0.1294(2)	0.0772(2)	0.1545(2)	90.04(9)	64.00(9)	90.70(9)	720.5
JC-1iz	8.574(9)	13.008(9)	7.207(9)	90	116.01(9)	90	0.1298(1)	0.0769(1)	0.1544(2)	90	63.99(9)	90	722.4
JC-2iz	8.580(4)	12.973(5)	7.211(4)	90.35(4)	115.95(3)	89.04(4)	0.1296(1)	0.0771(1)	0.1542(1)	90.08(5)	64.05(4)	90.90(4)	721.6
D-1nz	8.580(6)	12.977(8)	7.210(6)	90.35(7)	115.95(5)	89.07(6)	0.1296(1)	0.0771(1)	0.1542(1)	90.06(7)	64.05(5)	90.86(5)	721.7
D-2nz	8.577(9)	12.958(9)	7.212(6)	90.28(8)	115.96(5)	89.01(8)	0.1297(1)	0.0772(1)	0.1542(1)	90.17(8)	64.04(5)	90.96(8)	720.6
D-3nz	8.568(9)	12.968(9)	7.214(7)	90.36(9)	116.02(6)	88.63(9)	0.1299(1)	0.0771(1)	0.1543(1)	90.27(8)	63.98(6)	91.34(9)	720.1
D-4nz	8.579(9)	12.960(9)	7.207(8)	90.19(9)	115.92(9)	88.93(9)	0.1296(2)	0.0772(1)	0.1543(1)	90.30(9)	64.08(9)	91.10(9)	720.6
D-5nz	8.580(9)	12.977(9)	7.211(9)	90.12(9)	115.94(8)	89.21(9)	0.1296(1)	0.0771(1)	0.1542(2)	90.26(9)	64.06(9)	90.82(7)	721.9
D-6nz	8.571(7)	12.965(6)	7.211(5)	90.26(4)	115.97(4)	89.16(4)	0.1298(1)	0.0771(1)	0.1543(1)	90.12(4)	64.03(4)	90.81(4)	720.3
D-7nz	8.575(9)	12.990(9)	7.213(6)	90.44(9)	115.90(6)	89.08(8)	0.1297(1)	0.0770(1)	0.1541(1)	89.96(9)	64.10(6)	90.81(8)	722.7
U-1iz	8.564(9)	12.969(9)	7.198(6)	90.08(9)	115.83(9)	89.25(9)	0.1297(1)	0.0771(1)	0.1543(2)	90.27(9)	64.17(9)	90.80(7)	719.5
U-2iz	8.571(9)	12.972(9)	7.210(7)	90.30(8)	115.90(7)	89.00(9)	0.1297(2)	0.0771(1)	0.1542(1)	90.15(8)	64.10(7)	90.97(9)	721.0
LM-1iz	8.585(9)	12.973(9)	7.206(9)	90.28(9)	116.00(9)	89.25(9)	0.1296(1)	0.0771(1)	0.1544(2)	90.06(9)	64.00(9)	90.72(9)	721.2
C-1nz	8.575(9)	12.956(9)	7.208(8)	90.30(7)	115.82(8)	89.02(8)	0.1296(2)	0.0772(1)	0.1541(2)	90.14(6)	64.18(8)	90.95(7)	720.7
T-1nz	8.568(9)	13.016(9)	7.210(9)	90.25(9)	115.89(9)	89.12(9)	0.1298(1)	0.0768(1)	0.1542(1)	90.15(9)	64.11(9)	90.86(9)	723.2
TA-1nz	8.573(9)	12.967(9)	7.217(8)	90.24(9)	115.95(9)	89.12(9)	0.1297(2)	0.0771(2)	0.1541(2)	90.16(9)	64.05(9)	90.86(9)	721.2
TAR-1nz	8.580(8)	12.952(9)	7.211(8)	90.21(9)	115.97(8)	89.07(9)	0.1297(2)	0.0772(1)	0.1542(2)	90.23(9)	64.03(8)	90.94(9)	720.3
VA-1nz	8.582(8)	12.940(8)	7.209(8)	89.93(9)	116.16(8)	89.16(9)	0.1297(1)	0.0773(1)	0.1544(1)	90.49(9)	63.94(8)	90.97(8)	719.1
VAG-1nz	8.578(9)	12.947(9)	7.210(8)	90.12(9)	115.88(6)	89.12(9)	0.1296(1)	0.0772(1)	0.1542(1)	90.29(9)	64.12(6)	90.92(9)	720.4
VD-1iz	8.578(9)	12.963(8)	7.207(9)	90.26(6)	116.02(7)	89.05(8)	0.1297(1)	0.0772(1)	0.1544(2)	90.18(7)	63.98(7)	90.93(8)	720.0
AL-1nz	8.571(9)	12.963(9)	7.211(8)	90.26(9)	115.98(9)	88.97(9)	0.1298(2)	0.0772(1)	0.1543(2)	90.21(9)	64.02(9)	91.03(9)	720.1
FO-1nz	8.526(9)	12.993(9)	7.225(9)	90.37(9)	115.82(9)	88.82(9)	0.1303(2)	0.0770(2)	0.1538(2)	90.16(9)	64.18(9)	91.13(9)	720.3

Sample legend: CS: Cerro de la Sal, PG: Peña Grajera, JC: Juan Calvillo, D: Diéresis, U: Umbría, LM: Los Mo
C: Coma, T: Traviesas I, TA: Traviesas II, TAR: Taravilla, VA: Valverda, VAG: Mina Barita, VD: Valdenoque
Alameda, FO: Fuenteobejuna; bz: border zone, wz: wall zone, iz: intermediate zone, cz: central zone, nz: no zon
N = Lines used in refinements.
Numbers in parentheses are the standard deviation of the digits to their immediate left.

perthite deduced from *a* and *V* is listed in Table 5. Note the high proportion of the Or component (>90%) in the potassic phase.

Feldspar Geochemistry

The results of the chemical analyses of the different feldspars are given in Table 6. Figures 12 and 13 show the concentrations of selected elements. For our comments on the chemical aspects, we have followed the interpretations of Smith (1974, 1983) and Shmakin (1979).

In terms of the ternary system Or–Ab–An, the successive generations of perthitic K-feldspar show a progressive decrease in Or and An and an increase in Ab (Fig. 14). The alkali elements change regularly throughout the zonal crystallization of the pegmatite (Fig. 2). Thus from border to center of a pegmatite body, and the K/Na ratio decrease, *i.e.*, Na increases.

In K-feldspar, Ti and Fe contents are low, partic in the case of Ti (<0.01%), whereas Fe appe somewhat larger quantities but likely in discrete m phases, reaching values of 0.05% in some sample plagioclase also shows low Ti contents (up to 0.(although somewhat higher than in the K-fel whereas the levels of Fe are much higher th K-feldspar (Table 6, columns 2, 3). On the other the P content, which reaches 0.73 wt% P_2O_5 in so the K-feldspar, is highest in those grains having the strongly microperthitic character (Fig. 12); such co trations are sufficient to take on petrogenetic si cance, in accordance with the findings of Černý (1985). The concentration of P increases from (border) to later (internal) generations, its concent

TABLE 3. TRICLINICITY AND Al/Si DISTRIBUTION IN POTASSIC FELDSPAR

SAMPLE	TRICLINICITY (Δ)		Al/Si DISTRIBUTION (b-c* and α-γ* plot)				
	(I)	(II)	Σt_1	Δt_1	t_1o	t_1m	$2t_2$
CS-1bz	0.32	0.36	0.866	0.389	0.627	0.239	0.134
CS-1wz	0.25	0.30	0.812	0.269	0.541	0.271	0.188
CS-1iz	0.44	0.27	0.843	0.194	0.519	0.324	0.157
CS-2iz	0.77	0.53	0.886	0.473	0.679	0.207	0.114
PG-1bz	0.94	0.59	1.000	0.524	0.762	0.238	0.000
PG-2bz	0.81	0.45	0.942	0.452	0.697	0.245	0.058
PG-1cz	0.78	0.23	0.730	0.243	0.487	0.244	0.270
PG-2cz	0.00	0.00	0.668	0.000	0.334	0.334	0.342
PG-3cz	0.91	0.93	1.000	0.899	0.949	0.051	0.000
JC-1bz	0.88	0.90	1.000	0.916	0.958	0.042	0.000
JC-2bz	0.37	0.34	0.912	0.330	0.621	0.291	0.088
JC-1wz	0.97	0.31	0.939	0.327	0.633	0.306	0.061
JC-1iz	0.00	0.00	0.748	0.000	0.394	0.394	0.212
JC-2iz	0.29	0.39	0.908	0.411	0.660	0.249	0.091
D-1nz	0.84	0.38	0.894	0.399	0.647	0.248	0.105
D-2nz	0.56	0.42	0.967	0.421	0.694	0.273	0.033
D-3nz	0.51	0.59	0.920	0.583	0.751	0.169	0.080
D-4nz	0.51	0.48	0.946	0.455	0.700	0.246	0.054
D-5nz	0.61	0.36	0.900	0.334	0.617	0.283	0.100
D-6nz	0.50	0.35	0.932	0.359	0.645	0.287	0.068
D-7nz	0.33	0.35	0.876	0.397	0.637	0.240	0.123
U-1iz	0.57	0.35	0.894	0.318	0.606	0.288	0.106
U-2iz	0.43	0.42	0.924	0.429	0.676	0.248	0.076
LM-1iz	0.54	0.31	0.868	0.323	0.596	0.272	0.132
C-1nz	0.50	0.41	0.992	0.420	0.706	0.286	0.008
T-1nz	0.45	0.38	0.774	0.377	0.575	0.198	0.227
TA-1nz	0.49	0.38	0.961	0.374	0.668	0.293	0.039
TAR-1nz	0.92	0.41	0.980	0.397	0.689	0.291	0.020
VA-1nz	0.84	0.42	0.977	0.352	0.664	0.313	0.023
VAG-1nz	0.78	0.40	1.000	0.371	0.686	0.314	0.000
VD-1iz	0.61	0.41	0.902	0.403	0.653	0.249	0.098
AL-1nz	0.75	0.45	0.936	0.441	0.688	0.248	0.064
FO-1nz	0.45	0.49	0.952	0.505	0.729	0.223	0.048

Sample legend: CS: Cerro de la Sal, PG: Peña Grajera, JC: Juan Calvillo, D: Diéresis, U: Umbría, LM: Los Morales, C: Coma, T: Traviesas I, TA: Traviesas II, TAR: Taravilla, VA: Valverda, VAG: Mina Barita, VD: Valdenoque, AL: Alameda, FO: Fuenteobejuna; bz: border zone, wz: wall zone, iz: intermediate zone, cz: central zone, nz: no zonation.
(I) : Δ = 12.5 (d_{131} - $d_{1\bar{3}1}$) (Goldsmith & Laves 1954).
(II): Δ = measured γ* - 90°/2.29° (McGregor & Ferguson 1989).
Al/Si distribution: Kroll & Ribbe (1987).

TABLE 4. Al-Si DISTRIBUTION IN TETRAHEDRAL POSITIONS ACCORDING & RIBBE (1987)

SAMPLE	({110} vs {1$\bar{1}$0} corrected translations)						
	Σtr_{ov}	Δtr_{ov}	Σt_1	Δt_1	t_1o	t_1m	2t
CS-1bz	15.567	0.113	0.867	0.389	0.628	0.239	0.
CS-1wz	15.575	0.080	0.815	0.275	0.545	0.270	0.
CS-1iz	15.570	0.060	0.841	0.206	0.523	0.317	0.
CS-2iz	15.564	0.140	0.888	0.482	0.685	0.203	0.
PG-1bz	15.545	0.156	1.000	0.535	0.767	0.233	0.
PG-2bz	15.556	0.133	0.936	0.456	0.696	0.240	0.
PG-1cz	15.586	0.071	0.740	0.244	0.492	0.248	0.
PG-2cz	15.598	0.000	0.658	0.000	0.329	0.329	0.
PG-3cz	15.536	0.263	1.000	0.902	0.951	0.049	0.
JC-1bz	15.543	0.267	1.000	0.917	0.958	0.042	0.
JC-2bz	15.560	0.097	0.904	0.333	0.618	0.286	0.
JC-1wz	15.556	0.096	0.932	0.328	0.630	0.302	0.
JC-1iz	15.583	0.000	0.750	0.000	0.375	0.375	0.
JC-2iz	15.561	0.120	0.905	0.412	0.659	0.246	0.
D-1nz	15.563	0.117	0.892	0.400	0.646	0.246	0.
D-2nz	15.552	0.124	0.958	0.425	0.691	0.266	0.
D-3nz	15.559	0.171	0.921	0.587	0.754	0.167	0.
D-4nz	15.555	0.134	0.941	0.461	0.701	0.240	0.
D-5nz	15.562	0.099	0.895	0.340	0.617	0.278	0.
D-6nz	15.557	0.105	0.925	0.362	0.643	0.282	0.
D-7nz	15.566	0.115	0.875	0.395	0.635	0.240	0.
U-1iz	15.563	0.095	0.891	0.325	0.608	0.283	0.
U-2iz	15.559	0.126	0.919	0.431	0.675	0.244	0.
LM-1i	15.566	0.094	0.867	0.324	0.596	0.271	0.
C-1nz	15.549	0.123	0.978	0.422	0.700	0.278	0.
T-1nz	15.580	0.110	0.783	0.379	0.581	0.202	0.
TA-1nz	15.553	0.111	0.950	0.377	0.664	0.286	0.
TAR-1nz	15.550	0.117	0.969	0.402	0.685	0.284	0.
VA-1nz	15.550	0.106	0.967	0.363	0.665	0.302	0.
VAG-1nz	15.545	0.110	0.999	0.377	0.688	0.311	0.
VD-1iz	15.561	0.119	0.901	0.407	0.654	0.247	0.
AL-1nz	15.557	0.130	0.931	0.445	0.688	0.243	0.
FO-1nz	15.556	0.147	0.940	0.506	0.723	0.217	0.

Sample legend: see Table 3.

being considerably lower in the plagioclase than in the coexisting K-feldspar (as with the findings of London *et al.* 1990). There does not appear to be any correlation between the P and Ca contents, which indicates that apatite microinclusions are not responsible for these values.

The B content of plagioclase tends to increase with An content of the plagioclase, and ranges from 13 to 35 ppm. The B contents of the K-feldspar are a bit lower (from <10 to 30 ppm), in agreement with the observations of Smith (1974). The plagioclase presents higher contents of Be (5 – 15 ppm) than the K-feldspar (3 – 5 ppm). These data agree with those given by Solodov (1958) for coexisting K-feldspar and plagioclase in four rare-metal pegmatites.

In the outcrops examined here (Table 6, Fig. 12), the concentrations of Rb and Cs of both the K-feldspar and plagioclase increase weakly inward, whereas those of Sr and Ba decrease, which agrees with the hypotheses of Shmakin (1979) and Smith (1983). This is particularly noticeable in the case of Rb and in the K/Rb ratio (Fig. 13), which varies from 66 in the border areas to 121 in the internal zone. These findings parallel those published by Černý *et al.* (1985). In four samples in which K-feldspar and plagioclase coexist, the Rb, Cs and, to a lesser extent, Ba contents are seen to be strongly

partitioned in the K-feldspar over the coexisting pla clase (*cf.* Černý *et al.* 1984).

According to Černý *et al.* (1985), the Rb conte K-feldspar decreases after the crystallization of major zones and during later metasomatic altera This finding would explain the low Rb content fou one sample from the Diéresis quarry (D–4nz), wher metasomatic overprint is quite clear. As menti

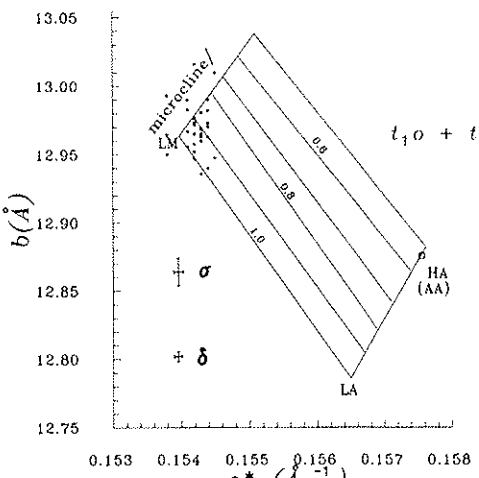

FIG. 6. Plot of $b - c^{\circ}$ used for determining ($t_1o + t_1m$) in tr K-feldspar with $t_1o \neq t_1m$. Theoretical end-member low microcline, HA high albite, AA analbite, LA low (Kroll & Ribbe 1987); σ: maximum error ($\Delta\sigma_x$ = 0 $\Delta\sigma_y$ = 0.009), δ: minimum error ($\Delta\delta_x$ = 0.0001, 0.002).

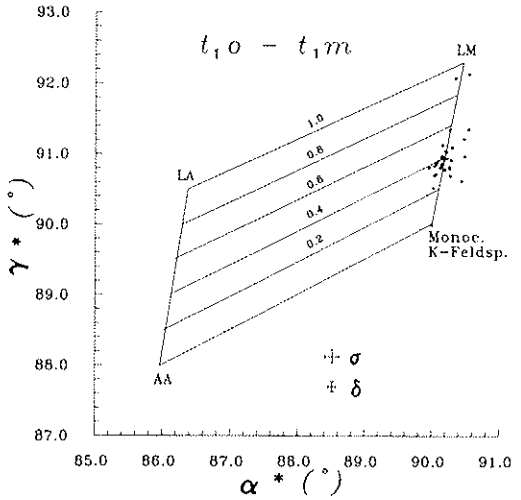

FIG. 7. Plot of $\alpha^* - \gamma^*$ used for determining $(t_1o - t_1m)$ in K-feldspar. Theoretical end-members: LA low albite, LM low microcline, AA analbite (Kroll & Ribbe 1987); σ: maximum error ($\Delta\sigma_x = 0.09$, $\Delta\sigma_y = 0.09$), δ: minimum error ($\Delta\delta_x = 0.04$, $\Delta\delta_y = 0.04$).

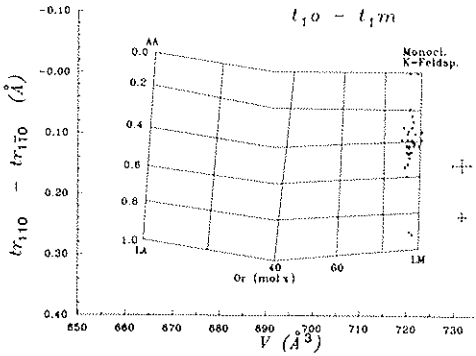

FIG. 8. Plot of $V - (tr_{110} - tr_{1\bar{1}0})$ used for determining $(t_1o$ and orthoclase content (Or mol%) in K-feldspar. The cal end-members: LA low albite, AA analbite, LM microcline, HS high sanidine (Kroll & Ribbe 198 maximum error ($\Delta\sigma_x = 2.1$, $\Delta\sigma_y = 0.013$), δ: minimum ($\Delta\delta_x = 0.9$, $\Delta\delta_y = 0.006$).

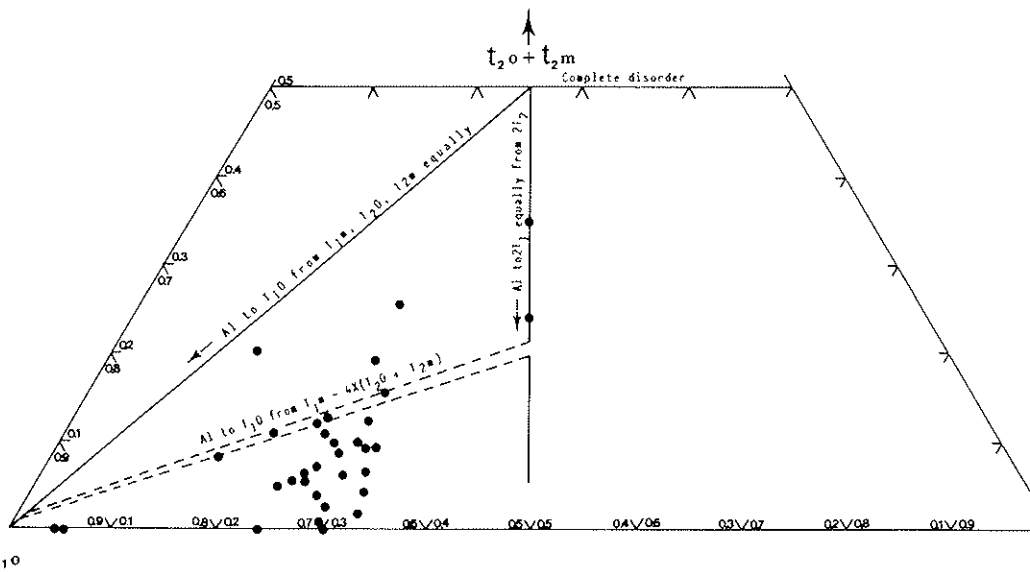

FIG. 9. Triangular plot of the distribution of Al in tetrahedral sites in K-feldspar specimens in the manner of Stewart & W (1974, Fig. 8). The path of Al–Si ordering in some of those authors' sodium feldspar, where the Al moves to t_1o in proportions from t_1m, t_2o and t_2m, is indicated by the continuous line starting at the t_1o vertex. Samples of interm microcline are ordered according to the model in which the Al moves to t_1o from t_1m approximately four times faste from t_2o and t_2m (dotted lines). The straight vertical line, along which $t_1o = t_1m$, represents monoclinic feldspar. All pa ordering are taken from Stewart & Wright (1974).

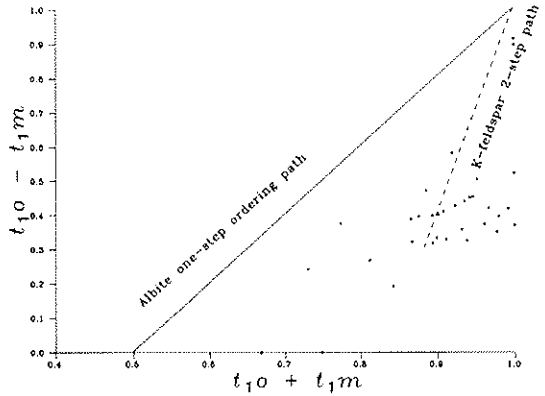

FIG. 10. Plot of $(t_1o + t_1m)$ *versus* $(t_1o - t_1m)$ for K-feldspar showing one-step and two-step ordering paths in alkali feldspar (Eggleton & Buseck 1980).

above, the Sr content of both feldspars decreases (Fig. 12) as crystallization of the pegmatitic units proceeds (Shmakin 1979). It must be pointed out that all the feldspars from the Diéresis quarry present Sr contents of more than 100 ppm. The Cs values are normal for feldspars from pegmatitic outcrops, according to the data of Smith (1974). The Ba content of the K-feldspar sho a slight decrease from border to center of the pegma This is also clear in the Ba/Rb ratio, which varies fr 188 for the border zone to 249 in the internal zone of pegmatite. Similar data also were given by Shma (1979) and Černý *et al.* (1984).

The Pb, as in most feldspars (Smith 1974), shows definite pattern of behavior. Attention should be dra to the high U content, which can reach 16 ppm in central zones of the Cerro de la Sal quarry. These va are much higher than those given by Smith (1974), suggested that they may be present as impurities. Th content is clearly lower than the data reported by (1962). Finally, the Au values (up to 6 ppm in Diér and 5 ppm in Peña Grajera) are slightly higher than th given by Tilling *et al.* (1973) as normal for gra pegmatites.

Cluster and correlational statistical analyses w carried out to study the relation between the struct and chemical parameters (Table 7, Fig. 15). The res of these analyses (Table 7) show values coherent the other observations made and reveal the importa of Al_2O_3, which is closely connected to the cell para ters (c, α, γ) of the K-feldspar, and also to the distribu parameters (t_1o, t_1m, $2t_2$). The values obtained for I show identical results, due to its behavior parallel to

TABLE 5. INTERNAL STRAIN INDEX AND CONTENT OF ORTHOCLASE COMPONENT IN PERTHITIC FELDSPAR

SAMPLE	I		II					
	Δa	S.I.	1	2	3	4	5	6
CS-1bz	+ 0.058	- 2.887	0.9539	0.9644	0.9565	0.9656	0.9682	0.9626
CS-1wz	+ 0.054	+ 1.819	0.9580	0.9681	0.9607	0.9698	0.9726	0.9635
CS-1iz	+ 0.056	+ 1.986	0.9394	0.9501	0.9425	0.9509	0.9537	0.9540
CS-2iz	+ 0.096	+ 5.584	0.9324	0.9428	0.9355	0.9441	0.9469	0.9689
PG-1bz	+ 0.076	+ 3.482	0.9072	0.9182	0.9111	0.9186	0.9211	0.9940
PG-2bz	- 0.063	- 5.310	0.9286	0.9392	0.9323	0.9399	0.9429	0.9500
PG-1iz	- 0.071	- 9.672	0.9498	0.9604	0.9529	0.9614	0.9643	0.9296
PG-2iz	- 0.063	- 8.803	0.9399	------	0.9432	0.9519	0.9295	0.9118
PG-3iz	- 0.071	- 3.486	0.9309	0.9417	0.9342	0.9425	0.9450	0.9296
JC-1bz	- 0.074	- 10.890	0.9455	0.9562	0.9482	0.9573	0.9600	0.9206
JC-2bz	- 0.049	- 10.047	1.0000	1.0000	1.0000	1.0000	1.0000	0.9890
JC-1wz	+ 0.154	+ 11.503	0.9285	0.9389	0.9319	0.9402	0.9428	1.0000
JC-1iz	- 0.060	- 11.208	0.9847	------	0.9858	0.9955	0.9180	0.9181
JC-2iz	- 0.054	- 2.437	0.9603	0.9705	0.9628	0.9719	0.9746	0.9735
D-1nz	- 0.055	- 3.169	0.9638	0.9739	0.9658	0.9752	0.9780	0.9727
D-2nz	+ 0.048	+ 1.353	0.9314	0.9425	0.9349	0.9432	0.9455	0.9659
D-3nz	- 0.066	- 3.498	0.9180	0.9285	0.9215	0.9298	0.9320	0.9409
D-4nz	+ 0.075	+ 3.566	0.9313	0.9420	0.9346	0.9429	0.9454	0.9702
D-5nz	- 0.054	- 3.757	0.9700	0.9799	0.9722	0.9814	0.9845	0.9729
D-6nz	+ 0.022	- 0.405	0.9235	0.9343	0.9272	0.9352	0.9378	0.9497
D-7nz	- 0.059	- 9.277	0.9933	1.0000	0.9938	1.0000	1.0000	0.9605
U-1iz	+ 0.082	+ 4.705	0.9027	0.9133	0.9065	0.9147	0.9165	0.9307
U-2iz	- 0.008	- 1.811	0.9437	0.9542	0.9464	0.9556	0.9581	0.9516
LM-1iz	+ 0.040	+ 0.830	0.9496	0.9600	0.9524	0.9615	0.9642	0.9863
C-1nz	+ 0.080	+ 4.046	0.9360	0.9467	0.9392	0.9479	0.9502	0.9608
T-1nz	- 0.066	- 15.773	1.0000	1.0000	1.0000	1.0000	1.0000	0.9409
TA-1nz	- 0.062	- 4.022	0.9490	0.9595	0.9518	0.9606	0.9636	0.9537
TAR-1nz	+ 0.080	+ 3.951	0.9248	0.9355	0.9282	0.9369	0.9390	0.9732
VA-1nz	+ 0.127	+ 8.985	0.8913	0.9018	0.8951	0.9028	0.9045	0.9798
VAG-1nz	+ 0.099	+ 5.944	0.9249	0.9355	0.9283	0.9366	0.9390	0.9689
VD-1iz	+ 0.068	+ 2.893	0.9163	0.9272	0.9199	0.9276	0.9302	0.9681
AL-1nz	+ 0.031	+ 0.173	0.9182	0.9290	0.9224	0.9304	0.9324	0.9505
FO-1nz	- 0.108	- 20.032	0.9241	0.9348	0.9277	0.9360	0.9385	0.8324

I. Internal strain indexes: Δa = after Stewart & Wright (1974). S.I. = after Kroll & Ribbe (1987).
II. Solid solution composition in K-feldspar from X-ray data following the models of
1) Waldbaum & Thompson (1968) (compositions estimated from cell volume).
2) Kroll & Ribbe (1983) (compositions estimated from cell volume for K-feldspar with structural state intermediate or completely unknown).
3) Kroll & Ribbe (1983) (compositions estimated from cell volume for LA-LM series).
4) Kroll *et al.* (1986) (compositions estimated from cell volume).
5) Hovis (1986) (compositions estimated from cell volume).
6) Hovis (1986) (compositions estimated from *a* axis).
Sample legend: see Table 3.

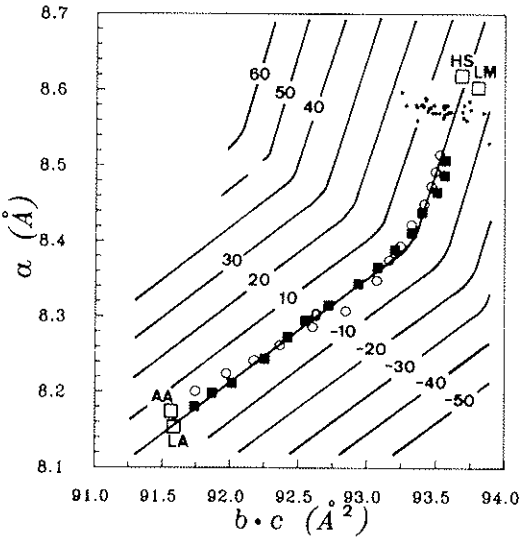

FIG. 11. Strain index (S.I.) in K-feldspar (Kroll & 1987). Unstrained K-feldspar: LA–LM series squares). AA–HS series (open circles). This study: isks.

of Al. Thus the tendencies toward the center o pegmatitic body would indicate an increase in th value and a decrease of t_1m and $2t_2$. It seems clea there is a high degree of correlation between struc and chemical parameters, and we may therefore con the possibility of evolution toward increasingly or members, with a higher degree of triclinicity i successive generations of feldspar that appear.

In order to characterize the different types of pe tites and estimate their potential for mineralizatio have represented the values of K/Cs *versus* Na_2O a Gordiyenko (1971, 1976) (Fig. 16). All the K-fel samples examined plot in the field of the rare- pegmatites and, within this field, most are represen the area of pegmatites with Li minerals (excep K-feldspar from the Peña Grajera quarry, which the field of pegmatites with Li, Be and Ta mineral

TABLE 6. CHEMICAL ANALYSES OF MAJOR ELEMENTS AND TRACE ELEMENTS IN PERTHITIC K-FELDSPAR AND PLAGIOCLASE

	CS-1bz	CS-1wz	CS-1iz	CS-2iz	PG-2bz	PG-1cz	PG-3cz	JC-1bz	D-3nz	D-4nz	CS-2bz	CS-2wz	D-3nz	D-
SiO_2	64.10	64.20	63.80	64.50	64.70	65.30	65.10	64.80	64.60	64.90	65.70	65.20	64.40	6
TiO_2	0.01	0.01	0.01	0.01	0.00	0.00	0.00	0.01	0.01	0.01	0.02	0.02	0.02	
Al_2O_3	19.40	19.60	19.60	19.40	19.20	19.30	19.20	19.00	19.10	19.00	20.90	20.60	21.50	2
Fe_2O	0.02	0.01	0.01	0.01	0.02	0.05	0.03	0.05	0.05	0.05	0.03	0.03	0.13	
MgO	0.10	0.10	0.11	0.10	0.09	0.10	0.09	0.10	0.11	0.11	0.10	0.11	0.13	
CaO	0.05	0.06	0.08	0.07	0.01	0.01	0.01	0.01	0.03	0.01	0.99	0.87	1.70	
Na_2O	2.92	3.54	3.18	3.68	2.98	3.33	3.28	2.99	2.62	2.58	11.10	11.00	10.20	1
K_2O	12.40	11.80	12.30	11.50	12.50	11.70	11.70	12.20	13.20	13.00	0.75	1.10	1.33	
P_2O_5	0.38	0.46	0.73	0.48	0.23	0.31	0.25	0.15	0.04	0.04	0.10	0.51	0.04	
LOI	0.31	0.31	0.39	0.39	0.62	0.39	0.39	0.47	0.31	0.39	0.77	0.62	0.70	
SUM	99.80	100.20	100.30	100.20	100.40	100.60	100.10	99.90	100.20	100.20	100.50	100.10	100.20	10
Or	73.45	68.46	71.50	67.07	73.41	69.79	70.10	72.86	76.76	76.85	4.04	5.92	7.24	
Ab	26.34	31.24	28.10	32.62	26.59	30.21	29.90	27.14	23.14	23.15	91.44	90.16	84.94	8
An	0.71	0.30	0.40	0.30	0.00	0.00	0.00	0.00	0.10	0.00	4.52	3.92	7.82	
B	10	10	23	16	10	10	10	10	30	10	35	19	13	3
Be	4	4	5	4	4	4	4	3	4	5	11	15	5	1
Rb	503	525	687	581	663	727	734	419	514	468	16	58	40	6
Cs	9	8	23	10	31	49	44	5	8	7	1	1	1	
Sr	25	29	22	10	52	15	25	62	138	160	82	10	184	30
Ba	209	260	205	241	205	102	149	590	523	696	111	127	179	29
Mn	18	17	13	15	16	19	14	13	20	11	23	39	26	3
Pb	26	22	20	18	16	12	12	24	22	18	14	12	8	1
U	<0.5	<0.5	16.8	<0.5	<0.5	<0.5	0.5	<0.5	<0.5	<0.5	0.5	0.9	12.5	
Y	<10	<10	<10	<10	<10	<10	<10	<10	12	<10	<10	<10	<10	<1
Au	<5	<5	<5	<5	5	<5	5	<5	6	<5	<5	<5	<5	<5

A) Chemical analyses from the X-Ray Assay Laboratories (Toronto, Ontario, Canada).
Mayor element compositions in wt %. Or, Ab & An content in mol %. Trace element compositions in ppm (Au in p
The four last column correspond to Na-feldspar analyses. Sample legend: see Table 3.

	CS-3bz	CS-3bz	PG-3bz	PG-3bz	PG-2cz	PG-2cz	PG-4cz	PG-4cz	D-10nz	D-10nz
SiO_2	68.98	63.24	67.92	63.46	67.63	63.43	66.71	63.91	64.70	63.50
TiO_2	n.d.	n.d.	0.02	0.00	0.02	0.00	n.d.	n.d.	0.00	0.00
Al_2O_3	19.15	18.51	19.75	18.76	19.46	18.57	19.93	18.73	21.51	18.25
Fe_2O	n.d.	n.d.	0.00	0.06	0.02	0.00	n.d.	n.d.	0.10	0.00
MnO	n.d.	n.d.	0.02	0.00	0.01	0.06	n.d.	n.d.	0.02	0.02
MgO	n.d.	n.d.	0.01	0.00	0.02	0.00	n.d.	n.d.	0.03	0.00
CaO	0.19	0.00	0.20	0.00	0.12	0.00	0.44	0.00	2.69	0.01
Na_2O	11.94	1.51	11.48	1.16	11.45	0.72	11.40	0.82	9.94	0.47
K_2O	0.18	15.23	0.15	15.92	0.13	16.46	0.15	15.99	0.28	17.11
P_2O_5	n.d.	n.d.	0.00	0.28	0.10	0.20	n.d.	n.d.	0.05	0.00
BaO	0.06	0.26	n.d.	n.d.	n.d.	n.d.	0.02	0.07	0.05	0.17
SUM	98.05	98.75	99.56	99.65	98.94	99.45	98.65	99.52	99.36	99.53
Or	1.47	90.98	1.27	93.21	1.11	95.81	1.25	95.12	2.17	97.27
Ab	96.99	9.02	97.04	6.79	97.86	4.19	95.08	4.88	76.99	2.67
An	1.54	0.00	1.69	0.00	1.03	0.00	3.67	0.00	20.84	0.06

B) Chemical analyses from Na and K-phase of the perthitic alkali feldspar by Electron Microprobe Analyses.
n.d. = not determinated. Sample legend: see Table 3.

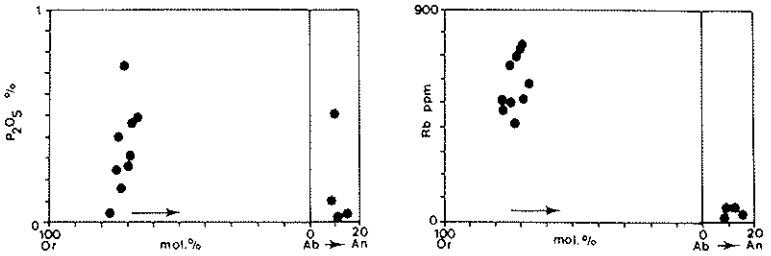

FIG. 12. Concentrations of P
Ba, Cs and Sr content v
compositional variations
feldspar and plagioclase.
ues of mol% Or are dec
from chemical data of Tab
The arrow indicates evol
toward the center of the pe
titic body.

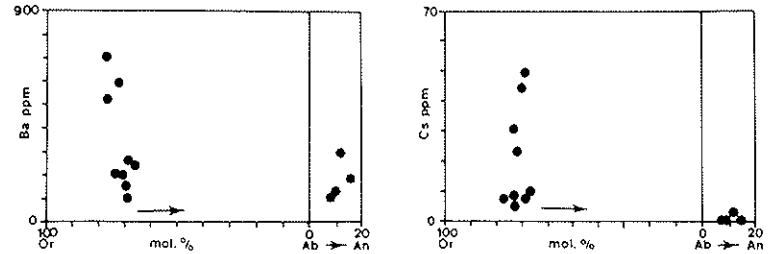

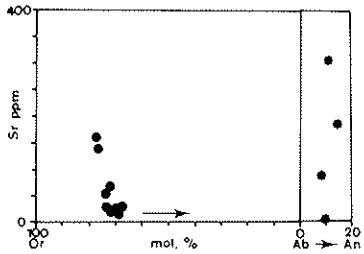

FIG. 13. Correlation plots bet
selected trace elements
feldspar (r = coefficient
ear correlation).

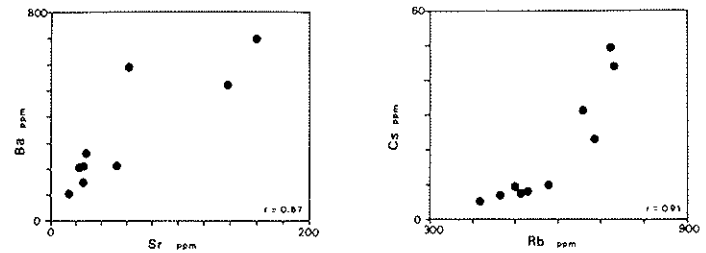

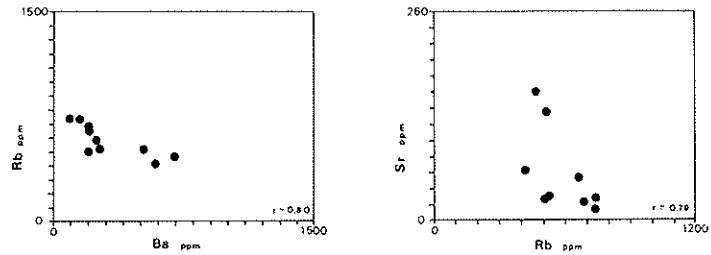

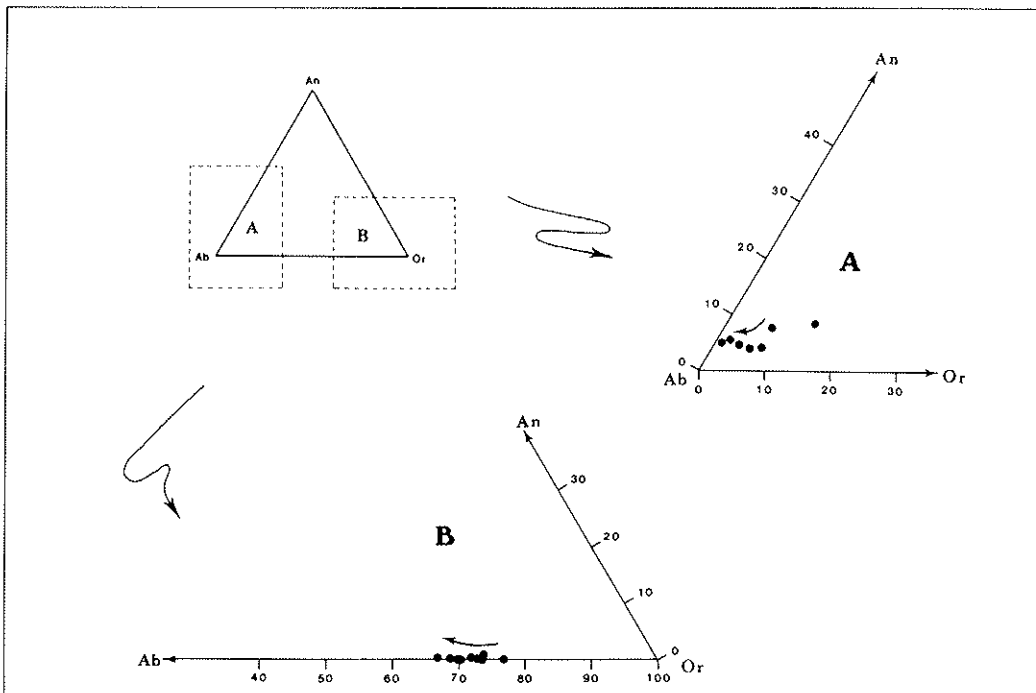

FIG. 14. Evolution of K-feldspar and plagioclase composition in the Or–Ab–An triangular plot. The arrow indicates evo toward the center of the pegmatitic bodies.

The temperatures resulting from the application of the two-feldspar geothermometer by Fuhrman & Lindsley (1988) gave a mean temperature of 500° ± 30°C.

PETROGENETIC INTERPRETATIONS

The feldspars in the Sierra Albarrana pegmatites show, to differing degrees, the development of stages of magmatic, subsolidus or postmagmatic, and hydrothermal or deuteric crystallization, according to the terminology of Parsons & Brown (1984).

Thermobarometry, using the biotite–garnet exchange and plagioclase – garnet – aluminum silicate – quartz equilibrium, led to González del Tánago & Peinado (1990) to estimate the metamorphic path in which the thermal peak is reached at 675° ± 25°C and 4.9 ± 0.5 kbar. These temperatures and pressures correspond to the upper amphibolite facies of regional metamorphism, where temperatures of 750° – 625°C were reached, producing partial fusion and migmatites. Under these conditions, the first K-feldspar to be formed is disordered and monoclinic (orthoclase). Except for two samples, disordered K-feldspar was not found. The metastable persistence of orthoclase in some pegmatitic bodies (Peña Grajera and Juan Calvillo) could refle development of the magmatic stage of Parsons & B (1984), and a relatively rapid decompression, v would have prevented the inversion to a triclinic spar. This uplift may be a consequence of the diste process that affected the region during the Herc orogeny (Quesada & Dallmeyer 1993) and proc deep fractures parallel to the axis of Sierra Alba These fractures aided the magmatic activity respor for the formation of the Los Pedroches batholit Villaviciosa – La Coronada complex, *etc.* (Delga *al.* 1985, Sánchez-Carretero *et al.* 1990). Although processes are not related genetically nor spatially pegmatites, they do indicate the existence of a diste process on a regional scale. This would explai prominence of low microcline (without orthocla these pegmatites compared to most granitic pegma In the remaining samples, the more ordered mono K-feldspar and triclinic K-feldspar result from ar ordering of the primary K-bearing feldspar, v occurred as temperature fell and in the presen alkali-rich solutions (Stewart & Wright 1974, Egg & Buseck 1980).

Al–Si ordering, inversion of monoclinic to tri symmetry (at approximately 500°C, according to B

TABLE 7. LINEAR CORRELATION–COEFFICIENTS BETWEEN STRUCTURAL AND CHEMICAL PARAMETERS OF K–FELDSPAR

	a	b	c	α	β	γ	Vol	t_1o	t_1m	$2t_2$	Δa	S.I.	SiO_2	TiO_2	Al_2O_3	Fe_2O_3	MgO	CaO	Na_2O	K_2O	P_2O_5	Or	Ab	An	B	Be	Rb	Cs	Sr	Ba	Mn	Pb
a	1.000																															
b	0.036	1.000																														
c	-0.618	-0.620	1.000																													
α	-0.615	-0.413	0.854	1.000																												
β	0.023	0.061	0.448	0.344	1.000																											
γ	0.556	0.736	-0.818	-0.792	0.018	1.000																										
Vol	0.235	0.493	-0.222	-0.024	0.073	0.308	1.000																									
T_1o	-0.480	-0.818	0.835	0.763	0.012	-0.991	-0.332	1.000																								
T_1m	0.656	0.572	-0.777	-0.823	0.034	0.969	0.187	-0.929	1.000																							
$2T_2$	0.212	0.952	-0.762	-0.573	-0.057	0.854	0.438	-0.915	0.700	1.000																						
Δa	0.861	0.099	-0.703	-0.663	-0.451	0.513	0.211	-0.464	0.587	0.254	1.000																					
S.I.	0.831	-0.154	-0.618	-0.719	-0.445	0.379	-0.129	-0.317	0.493	0.073	0.866	1.000																				
SiO_2	-0.507	-0.138	0.479	0.556	0.284	-0.453	-0.217	0.402	-0.533	-0.192	-0.618	-0.503	1.000																			
TiO_2	0.453	-0.040	-0.335	-0.223	-0.311	0.116	0.110	-0.085	0.179	-0.031	0.639	0.484	-0.644	1.000																		
Al_2O_3	0.403	0.555	-0.731	-0.754	-0.434	0.681	0.438	-0.698	0.627	0.661	0.515	0.436	-0.686	0.146	1.000																	
Fe_2O_3	-0.515	-0.091	0.480	0.626	0.398	-0.403	-0.220	0.369	-0.454	-0.216	-0.565	-0.571	0.708	-0.126	-0.830	1.000																
MgO	0.304	0.180	-0.413	-0.379	-0.063	0.358	-0.100	-0.339	0.392	0.226	0.411	0.359	-0.357	0.717	0.013	0.247	1.000															
CaO	0.548	0.287	-0.698	-0.713	-0.448	0.522	0.195	-0.512	0.532	0.407	0.712	0.652	-0.867	0.604	0.820	-0.753	0.368	1.000														
Na_2O	0.050	0.359	-0.426	-0.402	-0.519	0.197	0.344	-0.262	0.080	0.416	0.222	0.209	-0.097	-0.165	0.665	-0.615	-0.412	0.436	1.000													
K_2O	0.131	-0.308	0.230	0.168	0.490	-0.018	-0.402	0.096	0.122	-0.317	-0.068	0.000	-0.118	0.319	-0.491	0.438	0.547	-0.198	-0.943	1.000												
P_2O_5	0.294	0.438	-0.616	-0.741	-0.475	0.557	0.382	-0.567	0.526	0.519	0.501	0.391	-0.669	0.140	0.922	-0.814	0.016	0.793	0.676	-0.548	1.000											
Or	-0.011	-0.358	0.390	0.356	0.525	-0.163	-0.368	0.231	-0.038	-0.403	-0.194	-0.165	0.062	0.195	-0.643	0.587	0.440	-0.398	-0.997	0.966	-0.665	1.000										
Ab	-0.016	0.346	-0.364	-0.327	-0.511	0.138	0.361	-0.209	0.011	0.390	0.163	0.136	-0.021	-0.227	0.614	-0.561	-0.467	0.358	0.994	-0.974	0.638	-0.999	1.000									
An	0.516	0.295	-0.502	-0.369	-0.264	0.454	0.399	-0.441	0.453	0.354	0.647	0.396	-0.817	0.516	0.683	-0.632	0.199	0.790	0.183	-0.082	0.626	-0.180	0.146	1.000								
B	0.074	-0.034	-0.203	-0.339	0.050	0.136	-0.469	-0.126	0.173	0.054	0.073	0.289	-0.399	0.401	0.140	-0.052	0.609	0.502	-0.156	0.367	0.158	0.198	-0.225	0.159	1.000							
Be	0.592	0.045	-0.520	-0.730	-0.118	0.583	-0.167	-0.516	0.690	0.243	0.550	0.668	-0.295	0.122	0.285	-0.214	0.504	0.301	-0.184	0.299	0.286	0.207	-0.228	0.177	0.265	1.000						
Rb	-0.207	0.217	-0.106	-0.332	0.004	0.229	-0.096	-0.258	0.169	0.314	-0.269	-0.073	0.205	-0.767	0.356	-0.267	-0.412	-0.033	0.428	-0.457	0.409	-0.441	0.450	-0.156	0.018	0.266	1.000					
Cs	-0.439	0.220	0.122	-0.010	0.136	0.050	-0.031	-0.099	-0.045	0.241	-0.517	-0.386	0.514	-0.918	0.073	0.059	-0.515	-0.390	0.280	-0.420	0.119	-0.314	0.338	-0.371	-0.235	0.066	0.915	1.000				
Sr	0.092	-0.409	0.254	0.247	0.338	-0.200	-0.455	0.259	-0.083	-0.408	-0.079	0.064	0.208	0.293	-0.691	0.640	0.536	-0.391	-0.845	0.869	-0.760	0.867	-0.864	-0.395	0.229	0.245	-0.532	-0.423	1.000			
Ba	0.040	-0.441	0.286	0.324	0.114	-0.365	-0.266	0.411	-0.260	-0.508	0.044	0.047	0.112	0.557	-0.682	0.591	0.551	-0.280	-0.673	0.673	-0.651	0.687	-0.686	-0.318	0.130	-0.007	-0.799	-0.678	0.861	1.000		
Mn	-0.133	0.530	-0.159	0.114	0.356	0.283	0.067	-0.347	0.139	0.517	-0.305	-0.315	0.008	-0.174	0.211	0.042	-0.083	0.099	0.067	0.001	-0.050	-0.055	0.055	0.212	0.232	-0.309	0.131	0.152	-0.156	-0.381	1.000	
Pb	0.239	-0.003	-0.064	0.098	-0.059	0.022	0.255	0.007	0.070	-0.092	0.342	0.088	-0.677	0.825	0.107	-0.128	0.413	0.446	-0.286	0.383	0.056	0.302	-0.329	0.608	0.207	-0.207	-0.796	-0.856	0.179	0.417	0.080	1.000

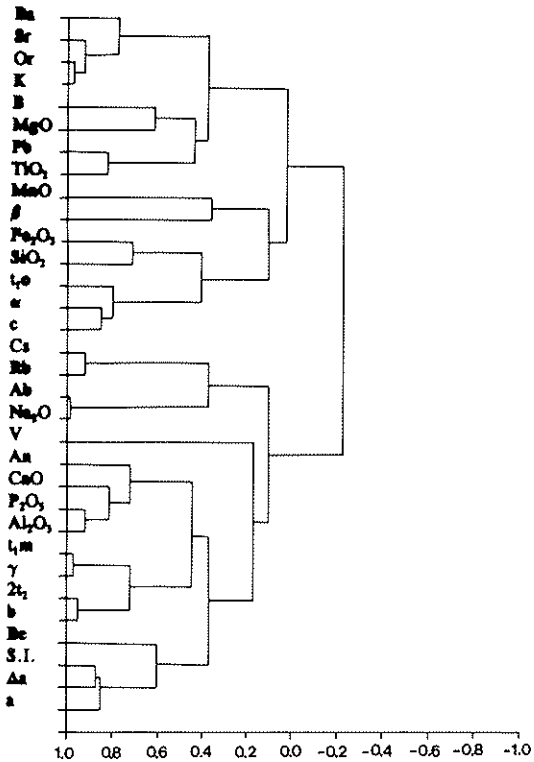

FIG. 15. Cluster analyses between the structural and chemical parameters of K-feldspar. The similarity criterion used is the coefficient of linear correlation.

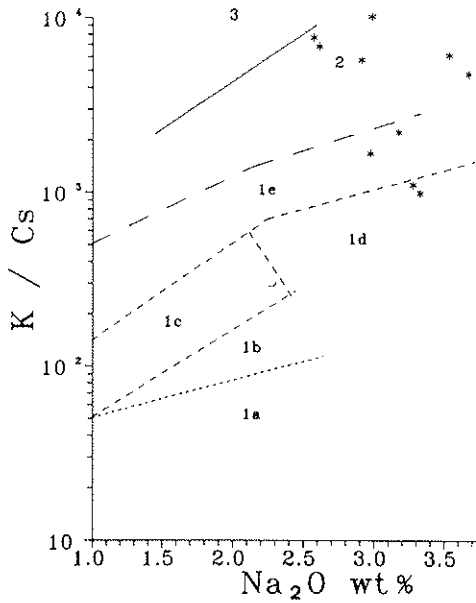

FIG. 16. Plot of K/Cs against Na_2O for K-feldspar of Ph zoic pegmatites. Continuous line: boundary betwe caceous pegmatites (3) and rare-element pegmatites (2). Broken lines: boundaries between different geoc cal series of rare-element pegmatites (1) containi minerals, (2) containing Li without Cs minerals, (1a, Li, Rb, Cs, Be, Ta minerals with pollucite; (1d) Li, minerals without pollucite; (1e) sterile bodies (Gord 1976). This study: asterisks.

& Parsons 1989) and formation of perthite took place at the subsolidus stage. As a result, a triclinic K-rich feldspar appeared, having an intermediate degree of Al–Si order (intermediate microcline), accompanied by the development of vein and braid perthites, as well as albite–pericline twinning (Fig. 5). This K-feldspar commonly is pink. The appearance of the tartan twinning in the microcline is proof of the existence of a monoclinic precursor. The subsolidus stage, which is widely represented in the feldspar populations examined here, persisted to temperatures as low as 400°C (Parsons & Brown 1984). The foregoing agrees with the temperature 500° ± 30°C resulting from the application of the two-feldspar geothermometer (Fuhrman & Lindsley 1988).

At temperatures below 400°C, the hydrothermal stage took place, with interactions between the feldspar and a fluid phase. The appearance of feldspar with a high degree of Al–Si order (close to the low microcline end-member) and the development of patch perthite (Fig. 5) are indicative of this stage, which is clearly represented in the Diéresis outcrop. This K-feldspar commonly is white.

ACKNOWLEDGEMENTS

Special thanks are due to Professor P. Keller (U sity of Stuttgart) for his constructive comment careful revision of the manuscript. Our thanks also F. Fontan (Université Paul Sabatier) for the fac provided to carry out the electron-microprobe ana This study was supported by Research Groups 4065 and 3179 of the "Junta de Andalucía" and P PS88–107 (DGICYT). This manuscript benefitte the careful revisions of Robert F. Martin, Rob Ferguson and Edward F. Duke.

REFERENCES

APPLEMAN, D.E. & EVANS, H.T., JR. (1973): Job 9214: in and least-squares refinement of powder diffractio *U.S. Geol. Surv., Comput. Contrib.* **20** (NTIS Doc **16188**).

AZOR, A., GONZALEZ LODEIRO, F., MARCOS, A. & SIM J.F. (1991): Edad y estructura de las rocas de

Albarrana (SW del macizo hespérico). Implicaciones regionales. *Geogaceta* **10**, 199-124.

BISH, D.L. & POST, J.E., eds. (1989): Modern Powder Diffraction. *Rev. Mineral.* **20**.

BORG, I.Y. & SMITH, D.K. (1969): Calculated X-ray powder patterns for silicate minerals. *Geol. Soc. Am., Mem.* **122**.

BROWN, W.L. & PARSONS, I. (1989): Alkali feldspars: ordering rates, phase transformations and behaviour diagrams for igneous rocks. *Mineral. Mag.* **53**, 25-42.

CARL, J.D. (1962): An investigation of minor element content of potash feldspar from pegmatites, Haystack Range, Wyoming. *Econ. Geol.* **57**, 1095-1115.

ČERNÝ, P., MEINTZER, R.E. & ANDERSON, A.J. (1985): Extreme fractionation in rare-element granitic pegmatites. Selected examples of data and mechanisms. *Can. Mineral.* **23**, 381-421.

_____, SMITH, J.V., MASON, R.A. & DELANEY, J.V. (1984): Geochemistry and petrology of feldspar crystallization in the Vezná pegmatite, Czechoslovakia. *Can. Mineral.* **22**, 631-651.

CHACÓN, J., DELGADO-QUESADA, M. & GARROTE, A. (1974): Sobre la existencia de dos diferentes dominios de metamorfismo regional en la banda Elvas – Badajoz – Córdoba (Macizo Hespérico Meridional). *Bol. Geol. Mineral.* **85**, 713-717.

CONTRERAS, M.C., GARROTE, A. & SANCHEZ-CARRETERO, R. (1983): Pegmatitas en materiales metamórficos del N de la provincia de Córdoba. Mineralogía y posibilidades económicas. *Cuad. Lab. Xeol. Laxe* **6**, 415-428.

DELGADO-QUESADA, M. (1971): Esquema geológico de la hoja nº de Azuaga (Badajoz). *Bol. Geol. Mineral.* **82**, 277-286.

_____, GARROTE, A. & SANCHEZ-CARRETERO, R. (1985): El magmatismo de la alineación La Coronada-Villaviciosa de Córdoba en su mitad oriental, zona de Ossa-Morena. *Temas Geol. IGME* **8**, 41-64.

_____, LIÑAN, E., PASCUAL, E. & PEREZ-LORENTE, F. (1977): Criterios para la diferenciación de dominios en Sierra Morena Central. *Studia Geologica* **12**, 75-90.

EGGLETON, R.A. & BUSECK, P.R. (1980): The orthoclase–microcline inversion: a high resolution transmission electron microscope study and strain analysis. *Contrib. Mineral. Petrol.* **74**, 123-133.

EGUILUZ, L. (1987): *Petrogénesis de las rocas ígneas y metamórficas en el antiforme Burguillos–Monesterio (Macizo ibérico meridional).* Tesis, Univ. Bilbao, Bilbao, Spain.

FUHRMAN, M.L. & LINDSLEY, D.H. (1988): Ternary-feldspar modeling and thermometry. *Am. Mineral.* **73**, 201-215.

GABALDÓN, V., GARROTE, A. & QUESADA, C. (1983): cuencas de Valdeinfierno y Benajarafe (Tournaisie Viseense). Caracterización sedimentológica e implic nes regionales. Dominio de Sierra Albarrana (Zon Ossa–Morena). *Comun. Serv. Geol. Portugal* **69**, 209-

GARROTE, A. (1976): Asociaciones minerales de m metamórfico de Sierra Albarrana (Provincia de Córd Sierra Morena Central. *Mem. Not. Publ. Mus. Lab. Mi Geol. Univ. Coimbra* **82**, 17-39.

_____, ORTEGA-HUERTAS, M. & ROMERO, J. (1980): yacimientos de pegmatitas de Sierra Albarrana (Prov de Córdoba). Sierra Morena. *Temas Geol. IGME*, 145

_____ & SÁNCHEZ-CARRETERO, R. (1983): Materiales vol clásticos en el carbonífero inferior al S–SW de Villavi de Córdoba (Zona de Ossa–Morena). *Comun. Serv. Portugal* **69**, 249-257.

GOLDSMITH, J.R. & LAVES, F. (1954): The microcline – san stability relations. *Geochim. Cosmochim. Acta* **5**, 1-1

GONZALEZ DEL TÁNAGO, J. & PEINADO, M. (1990): Contrib al estudio del metamorfismo de Sierra Albarrana (Z Córdoba, España). *Bol. Geol. Minero.* **101**, 678-700.

GORDIYENKO, V.V. (1971): Concentration of Li, Rb and potash feldspar and muscovite as criteria for assessir rare metal mineralization in granite pegmatites. *Int. Rev.* **13**, 134-142.

_____ (1976): Diagram for prediction and evaluati rare-metal mineralization in granitic pegmatite from ations in composition of potassic feldspars. *Dokl. Aca USSR, Earth Sci. Sect.* **228**, 149-151.

HOVIS, G.L. (1986): Behavior of alkali feldspars: cr lographic properties and characterization of compo and Al–Si distribution. *Am. Mineral.* **71**, 869-890.

KROLL, H. (1971): Determination of Al, Si distribution in feldspars from X-ray powder data. *Neues Jahrb. Mi Monatsh.*, 91-94.

_____ (1973): Estimation of the Al, Si distribution of felc from the lattice translations tr[110] and tr[1$\bar{1}$0]. I. feldspars. *Contrib. Mineral. Petrol.* **39**, 141-156.

_____ (1980): Estimation of the Al, Si distribution of feldspars from lattice translations tr[110] and tr Revised diagrams. *Neues Jahrb. Mineral. Monatsh.*,

_____ & RIBBE, P.H. (1983): Lattice parameters, compo and Al, Si order in alkali feldspars. *In* Feldspar Miner (P.H. Ribbe, ed.). *Rev. Mineral.* **2**, 57-99.

_____ & _____ (1987): Determining (Al, Si) distributio strain in alkali felspars using lattice parameters and di tion peak positions: a review. *Am. Mineral.* **72**, 491-

_____, SCHMIEMANN, I. & CÖLLN, G.V. (1986): Feldspar solutions. *Am. Mineral.* **71**, 1-16.

LONDON, D., ČERNÝ, P., LOOMIS, J.L. & PAN, J.J. (1990): Phosphorus in alkali feldspars of rare-element granitic pegmatites. *Can. Mineral.* **28**, 771-786.

MARTÍN-RAMOS, J.D. (1990): *Programa de Control y Análisis del Difractómetro de RX*. Dp. Legal M–11719, nº de registro: 08605.

MCGREGOR, C.R. & FERGUSON, R.B. (1989): Characterization of phases and twins in alkali feldspars by the X-ray precession technique. *Can. Mineral.* **27**, 457-482.

ORTEGA-HUERTAS, M., GARROTE, A., RODRIGUEZ-GORDILLO, J. & FENOLL, P. (1982): Pegmatitic assemblages in the metamorphic core of Sierra Albarrana (Córdoba, Spain). *Proc. 13th Gen. Meet., Int. Mineral. Assoc.* **41**, 641-650.

PARSONS, I. & BROWN, W.L. (1984): Feldspars and the thermal history of igneous rocks. *In* Feldspars and Feldspathoids (W.S. MacKenzie & W.L. Brown, eds.). *Reidel Publ. Co., NATO Adv. Study Inst., Ser.* C **137**, 317-371.

QUESADA, C., APALATEGUI, O., EGUILUZ, L., LIÑAN, E. & PALACIOS, T. (1990): Ossa-Morena zone: stratigraphy, Precambrian. *In* Premesozoic Geology of Iberia **1** (R.D. Dallmeyer & E. Martinez-García, eds.). Springer-Verlag, New York (252-258).

_____ & DALLMEYER, R.D. (1993): Tectonothermal evolution of the Badajoz-Córdoba shear zone (SW Iberia): characteristics and $^{40}Ar/^{39}$ Ar mineral age constraints. *Tectonophys.* (in press).

RIBBE, P.H. (1983a): Appendix: guides to indexing feldspar powder patterns. *In* Feldspar Mineralogy (P.H. Ribbe, ed.). *Rev. Mineral.* **2**, 325-341.

_____ (1983b): Chemistry, structure and nomenclature of feldspars. *In* Feldspar Mineralogy (P.H. Ribbe, ed.). *Rev. Mineral.* **2**, 1-19.

SANCHEZ-CARRETERO, R., EGUILUZ, L., PASCUAL, E. & C CEDO, M. (1990): Ossa-Morena zone: igneous roc Premesozoic Geology of Iberia **1** (R.D. Dallmeyer Martinez-García, eds.). Springer-Verlag, New York 313).

SHMAKIN, B.M. (1979): Composition and structure st K-feldspars from some U.S. pegmatites. *Am. Miner* 49-56.

SMITH, J.V. (1974): *Feldspar Minerals.* **2**. *Chemica Textural Properties.* Springer-Verlag, New York.

_____ (1983): Some chemical properties of feldspa Feldspar Mineralogy (P.H. Ribbe, ed.). *Rev. Mine* 281-296.

SOLODOV, N.A. (1958): Distribution of rare elements in als of rare-metal granitic pegmatites. *Geochemistry* 940.

STEWART, D.B. & WRIGHT, T.L. (1974): Al/Si orde symmetry of natural alkali feldspars, and the relation strained cell parameters to bulk composition. *Bul franç. Minéral. Cristallogr.* **97**, 356-377.

TILLING, R.I., GOTTFRIED, D. & ROWE, J.J. (1973): abundance in igneous rocks: bearing on gold mine tion. *Econ. Geol.* **68**, 168-186.

WALDBAUM, D.R. & THOMPSON, J.B., JR. (1968): M properties of sanidine crystalline solutions. II. Calcul based on volume data. *Am. Mineral.* **53**, 2000-2017.

WRIGHT, T.L. & STEWART, D.B. (1968): X-ray and optical of alkali feldspar. I. Determination of compositio structural state from refined unit-cell parameters a *Am. Mineral.* **53**, 38-87.

Received October 15, 1991, revised manuscript acc February 26, 1992.